SAR Image Registration Using An Improved Anisotropic Gaussian-SIFT Algorithm

Sourabh Paul
Department of Electronics and Communication Engineering,
National Institute of Technology,
Rourkela-769008, Odisha, India.
Email:sourabhpaul26@gmail.com

Umesh C. Pati
Department of Electronics and Communication Engineering,
National Institute of Technology,
Rourkela-769008, Odisha, India.
Email: ucpati@nitrkl.ac.in

***Abstract*— An Improved Anisotropic Gaussian-Scale Invariant Feature Transform (IAG-SIFT) algorithm is proposed to register the Synthetic Aperture Radar (SAR) images. The standard SIFT algorithm generates isotropic Gaussian scale space which blurs lots of details in the image. The Anisotropic Scale Space (ASS) can preserve more details than the isotropic one. However, in many SAR registration methods, the gradient calculation of the ASS is performed by using the simple differential equation which is not appropriate for SAR images. As the SAR images contain multiplicative speckle noise, simple difference operation is not suitable for gradient calculation. It can reduce the number of correct matches in SAR image registration. So, in this paper, a Gaussian-Gamma-Shaped Bi-Window (GGS-BW) is used for ratio based gradient computation which is very effective for SAR images. The proposed IAG-SIFT method significantly improves the matching performance between the SAR images. The Experimental results show the effectiveness of proposed IAG-SIFT algorithm in SAR image registration.**

Keywords— Synthetic Aperture Radar (SAR); Improved Anisotropic Gaussian-Scale Invariant Feature Transform (IAG-SIFT); Gaussian-Gamma-Shaped Bi-Window (GGS-BW).

I. INTRODUCTION

The main goal of the SAR (Synthetic Aperture Radar) image registration is to align the SAR images captured by the same or different sensors at different times and / or different view-points. In this process, a sensed SAR image is aligned with the reference SAR image. Unlike the optical sensors, the SAR sensors can capture the remote sensing images at the night and through the cloud also. This special ability of the SAR sensors makes it useful in the catastrophic event when the new data is compared with the old one to identify the changes. In such application, image registration is a very important step. Moreover, it finds many other applications such as image fusion and agricultural studies.

There are two types of SAR image registration methods: area-based methods and features-based methods. As the feature-based methods are computationally inexpensive, these are popularly used for SAR image registration. The feature-based image registration methods consist of the following steps: features extraction, feature matching, transformation parameter calculation using the position of matched features and transformation of the sensed image.

Scale-invariant feature transform (SIFT) [1] is an efficient feature-based method for remote sensing optical image registration [2]. The SIFT algorithm has five major steps. In the first step, the input images (reference and sensed images) are convolved with the Gaussian filter to generate the Gaussian scale space. Then, the difference of Gaussian (DOG) layers are formed by subtracting the adjacent scale layers. The extrema of the DOG layers are searched and these are regarded as the feature points. In the third step, single or multiple orientations are assigned for every feature point. Then, the descriptor of the feature point is generated by using the gradients of the local neighbors. Finally, feature matching is performed between the reference and sensed image features. However, the performance of standard SIFT algorithm is not satisfactory for SAR image registration. In standard SIFT algorithm, the gradients are computed by the simple differential equation. But, the simple differential equation is not an efficient gradient computation technique when the images are corrupted by the multiplicative speckle noise. Moreover, standard SIFT generates isotropic Gaussian scale space which blurs a lots of details in images.

Different modified version of the SIFT algorithm can be found in the literature of SAR image registration [3-7]. To reduce the effect of noise, Schwind et al. [3] presented a SIFT-OCT algorithm where the first octave of the scale space is skipped. However, it cannot produce sufficient correct matches in many SAR image pairs. Dellinger et al. [4] proposed a SAR-SIFT algorithm which is very effective to register SAR images captured by different view-points. However, the distribution of the SAR-SIFT feature is uneven. Later, in [5], a novel approach has been presented to uniformly distribute the SAR-SIFT features. In [6], a BF-SIFT algorithm is proposed, where the anisotropic scale space (ASS) is constructed by the bilateral filter (BF). But, the BF-SIFT is not an effectual approach to remove noise in the edge regions. In [7], an adapted anisotropic Gaussian (AAG)-SIFT algorithm is developed to reduce the effect of noise around the edges. Moreover, the ASS preserves more details than the Gaussian scale space (GSS). However, the gradients of the ASS-SIFT algorithm is computed by the simple differential equation which is not appropriate for SAR image. A proper gradient computation plays a significant role in the

matching performance of SAR image registration. The gradients computed by the simple differential equation can reduce the number of correct matches between the SAR images.

The SAR images contain multiplicative speckle noise where ratio based gradient computation is more effective. In literature, various ratio based operators can be found in [4] and [8] which are used for the edge detection in SAR images. The Gaussian-Gamma-Shaped Bi-Window (GGS-BW) [8], is an efficient ratio based edge detector which can minimize the false edge pixels near to the true edge. In [9], the GGS-BW based descriptor is used for optical-to-SAR image matching.

In this work, we have investigated the performance GGS-BW based ratio operator for SAR image registration. We have proposed an Improved Anisotropic Gaussian-Scale Invariant Feature Transform (IAG-SIFT) algorithm where the gradients are calculated by the GGS-BW based ratio operator. The proposed method can give better matching performance than the standard AAG-SIFT algorithm.

The paper is structured in different sections. Section II, provides the description of the standard AAG-SIFT method. In Section III, the proposed IAG-SIFT algorithm is presented. The simulation results have been presented in Section IV. The paper is concluded in Section V.

II. STANDARD AAG-SIFT METHOD

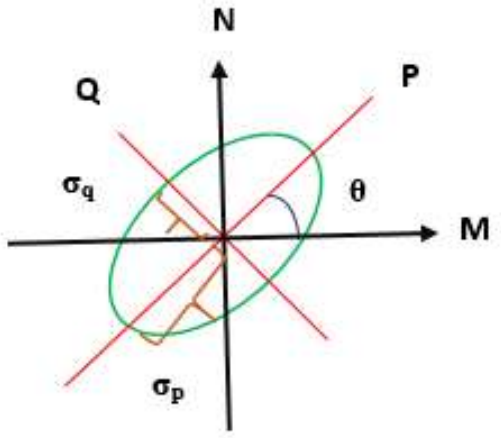

Fig. 1. Anisotropic Gaussian filter.

In standard AAG-SIFT method, the anisotropic scale space is generated by the anisotropic Gaussian filter (AGF) [10]. Fig. 1 shows an oriented AGF filter. The main working principle of the AGF is that it smooths the edge areas by the elliptical Gaussian mask, whereas the homogeneous areas are filtered by the radial mask. The oriented AGF is defined as:

$$F_\theta(p,q,\sigma_p,\sigma_q,\theta)=\frac{1}{2\pi\sigma_p\sigma_q}\exp\{-\frac{1}{2}\frac{p^2}{\sigma_p{}^2}\}*\exp\{-\frac{1}{2}\frac{q^2}{\sigma_q{}^2}\} \quad (1)$$

where "*" represents convolution; the direction of the filter is denoted by θ, $\sigma_p{}^2$ and $\sigma_q{}^2$ represent the scaling parameters in the p and q axis respectively. p-axis is directed in θ detection, whereas q-axis is orthogonal to θ, and

$$\begin{bmatrix} p \\ q \end{bmatrix}=\begin{bmatrix} \cos\theta & sin\theta \\ -sin\theta & \cos\theta \end{bmatrix}\begin{bmatrix} m \\ n \end{bmatrix} \quad (2)$$

Here, the value of σ_p is set equal to the scale parameter used for the Gaussian scale space formation. The value of σ_q is selected adaptively by calculating the second-moment matrix at the point.

The steps of the adapted anisotropic Gaussian (AAG) scale space formation proposed in [7] are as follows.

1. At every sample point, the orientation of the AGF filter is determined. The gradient orientations of the neighbors of the sample point are used to form an orientation histogram. The maximum peak of the histogram is considered as the direction of the gradient. The θ of the AGF is determined as orthogonal to the direction of the gradient.
2. In this step, the structure of the AGF is fixed. The value of the σ_p is calculated as

$$\sigma_p=\sigma_0 2^{\frac{o+l}{L}} \quad (3)$$

where σ_o is selected as 1.6. o and l present the indexes of octave and scale layer and L denotes the number of scale layers.

The value of σ_q is calculated by a second moment matrix M_s at each point. M_s is defined as

$$M_s=\begin{bmatrix} I_m^2(m,n) & I_mI_n(m,n) \\ I_mI_n(m,n) & I_n^2(m,n) \end{bmatrix} \quad (4)$$

where I_m and I_n are the derivatives at the sample point (m,n) in the M and N direction respectively. Simple differential equation is used to find the derivatives. The eigen values of the matrix M_s are used to calculate the value of isotropy (β_M) which provides the statistical characteristics around a local region. It is defined as

$$\beta_M=\frac{\lambda_m}{\lambda_M} \quad (5)$$

where λ_m and λ_M are the minimum and maximum eigen values of the matrix M_s respectively. The value of σ_q is computed as

$$\sigma_q=\sigma_p\beta^n \quad (6)$$

where the value of n is suggested as 1/3 in [7].

The ASS is constructed for the reference and the sensed SAR images. Then, SIFT features are extracted from the ASS. The descriptors are formed for each of the feature points by using the gradients of the local neighbors. Here also, simple differential equation is used to calculate the gradients. Finally, matching is performed between the feature descriptors of the reference and sensed images. The dual matching technique [6] is used to match

the features. But, some outliers exit in the matching pairs. The RANSAC (Random sample consensus) algorithm is implemented to remove the outliers.

III. Proposed IAG-SIFT Method

In our proposed IAG-SIFT algorithm, the ASS is constructed by following the same steps used in AAG-SIFT method. However, in our method, the gradients are computed in a different way. The determination of an accurate orientation of the AAG filter plays an important role as the smoothing is performed according to the orientation. The orientation of the AAG filter is determined by considering the gradients of the local neighbors. It is already mentioned that all the gradient computation of AAG-SIFT [7] is done by the simple differential equation which is not appropriate for the SAR images. So, in our proposed IAG-SIFT method, we have used a GGS-BW based ratio operator to compute the gradients. The GGS-BW contains two 2-dimensional windows which are defined as

$$W_U(m,n) = \frac{|n|^{\alpha-1}}{\sqrt{2\pi}\sigma_m \Gamma(\alpha)\beta^{\alpha}} \exp\{-(\frac{m^2}{2\sigma_m^2} + \frac{|n|}{\beta})\} \quad \text{for } n \geq 0 \tag{7}$$

$$W_L(m,n) = \frac{|n|^{\alpha-1}}{\sqrt{2\pi}\sigma_m \Gamma(\alpha)\beta^{\alpha}} \exp\{-(\frac{m^2}{2\sigma_m^2} + \frac{|n|}{\beta})\} \quad \text{for } n<0 \tag{8}$$

The shape of the windows is similar to the Gaussian function and the gamma function at the horizontal and vertical directions respectively. The window length is controlled by the parameter σ_m. The window width and the spacing between the windows are controlled by α and β respectively.

The two windows are oriented towards the vertical direction for each of the sample points. The local means for the two window functions are computed as

$$M_1(m,n) = \sum_{(m',n')} W_U(m',n') I(m-m', n-n') \tag{9}$$

$$M_2(m,n) = \sum_{(m',n')} W_L(m',n') I(m-m', n-n') \tag{10}$$

Then, the windows are oriented towards the horizontal direction and similarly, local means are computed for the two windows in this direction. Let, M_3 and M_4 are the local means in the horizontal direction.

Now, the horizontal and vertical gradients are calculated as

$$G_h = \log \frac{M_1(m,n)}{M_2(m,n)} \tag{11}$$

$$G_v = \log \frac{M_3(m,n)}{M_4(m,n)} \tag{12}$$

The gradient magnitude and orientation are computed as

$$G_M = \sqrt{G_h^2 + G_v^2} \tag{13}$$

$$G_\theta = \arctan \frac{G_v}{G_h} \tag{14}$$

Moreover, in our proposed method, GGS-BW based ratio operator is used to compute the gradients for descriptor construction.

IV. Experimental Result AnaLysis

In this section, the performance of the proposed IAG-SIFT algorithm is discussed. In order to verify the effectiveness, the performance of the proposed method is compared with the three SAR registration algorithms: SIFT-OCT [3], BF-SIFT [6] and AAG-SIFT [7].

As the effect of speckle noise is more significant in the first octave, the feature extraction is started from the second octave. The maximum value of o is set to 4. The value of L is taken as 4. In our experiments, the selected parameter values of the GGS-BW are α=2, β=0.5, σ_m=3.66 and the size of the window is taken as 9x9. The selected values give satisfactory results.

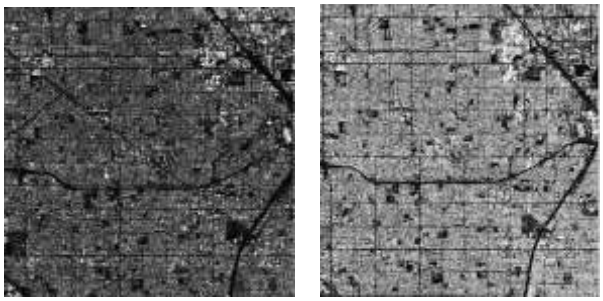

(a) (b)

Fig. 2. First data set consists of (a) Reference (size: 800x800 pixels) and (b) Sensed (size: 800x800 pixels) images.

Three data sets [11]-[12] are used to verify the performance of different methods. Fig. 2 shows the first data set. The images are captured by the Alos Palsar on 20/05/2008 and 11/01/2011 respectively over an area of South California. The images have significant illumination differences and these are corrupted by the speckle noise.

Fig. 3 shows the feature matching performance of these algorithms. From fig. 3 it can be seen that the proposed IAG-SIFT provides more matches than the other methods. Table I presents the qualitative assessment results for the different methods. It can be seen that the proposed method has the lowest RMSE value. The matching pairs obtained by the RANSAC, are used to compute the RMSE value [6]. As the proposed method gives more correct matches than other methods, the RMSE value is minimum in our method. The value of the mutual information computed between the register images is highest for the proposed method. The higher value of mutual information indicates better accuracy in registration. So, the registration accuracy is comparatively better in our method than the other algorithms.

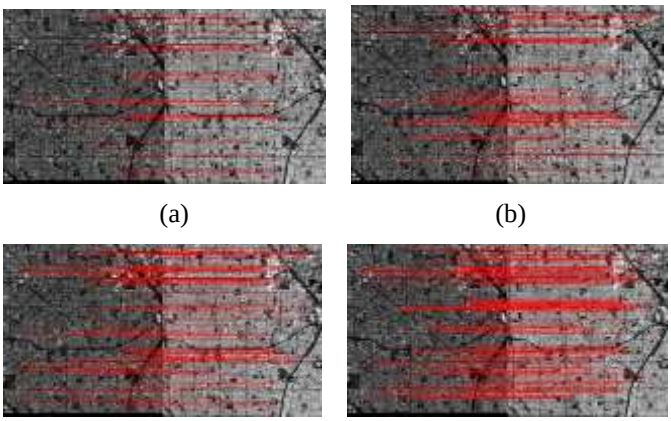

(a) (b)

(c) (d)

Fig. 3. Correct matches between the reference and sensed images. (a) SIFTOCT, (b) BF-SIFT, (c) AAG-SIFT and (d) IAG-SIFT.

TABLE I. QUALITATIVE ASSESSMENT

Method	Correct Matches	RMSE	MI
SIFT-OCT	28	1.102	0.319
BF-SIFT	48	0.96	0.362
AAG-SIFT	64	0.927	0.416
Proposed Method	**91**	**0.883**	**0.459**

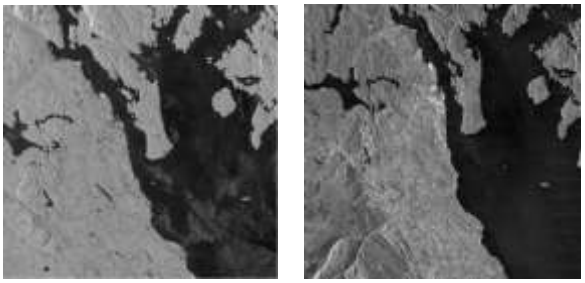

(a) (b)

Fig. 4. Second data set consists of (a) Reference (size: 800x800 pixels) and (b) Sensed (size: 800x800 pixels) images.

The second data set is shown in fig. 4. These images are captured by the Alos Palsar and TerraSAR-X sensors on 21/07/2010 and 05/06/2010 respectively covering the region of Campbell river. The images have scaling and orientational differences. The matching performance of the different algorithms is shown in fig. 5. Table II provides the comparative results of the algorithms. In this case also, the proposed method gives better performance than the other methods. However, the RMSE value is more than 1 which indicates that the sub-pixel accuracy is not obtained by the proposed method for the data set. As the matching pairs are not uniformly distributed over the images, the sub-pixel accuracy is not obtained.

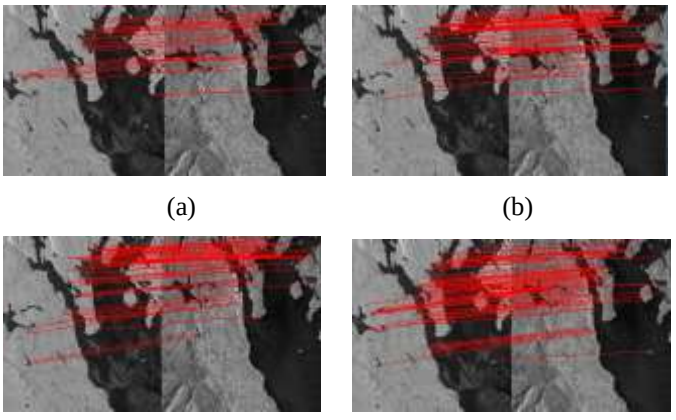

(a) (b)

(c) (d)

Fig. 5. Correct matches between the reference and sensed images. (a) SIFTOCT, (b) BF-SIFT, (c) AAG-SIFT and (d) IAG-SIFT

TABLE II. QUALITATIVE ASSESSMENT

Method	Correct Matches	RMSE	MI
SIFT-OCT	30	1.685	0.797
BF-SIFT	46	1.404	0.862
AAG-SIFT	57	1.383	0.882
Proposed Method	**72**	**1.207**	**0.924**

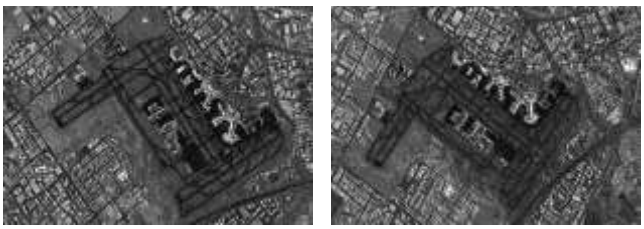

(a) (b)

Fig. 6. Third data set consists of (a) Reference (size: 500x750 pixels) and (b) Sensed (size: 500x750 pixels) images

The third data set is shown in fig. 6. The images are taken from the TerraSAR-X sensor on 18/09/2010 and 27/09/2010 respectively covering the area of Toronto. The images have significant view angle difference. Fig. 7 shows the feature matching results of the different methods. For this data set, the SIFT-OCT algorithm does not provide the correct correspondences. Therefore, the SIFT-OCT algorithm fails to register the images. Table III provides comparative results for the third data set. In this case also, the proposed method gives better results.

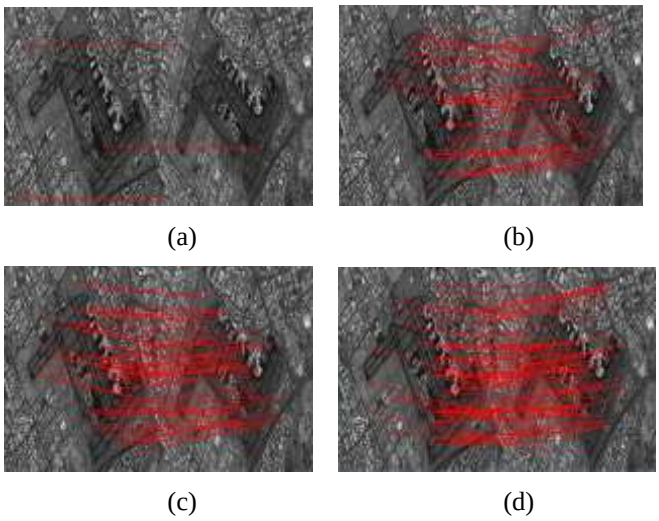

(a) (b) (c) (d)

Fig. 7. Correct matches between the reference and sensed images. (a) SIFTOCT, (b) BF-SIFT, (c) AAG-SIFT and (d) IAG-SIFT

TABLE III. QUALITATIVE ASSESSMENT

Method	Correct Matches	RMSE	MI
SIFT-OCT	-	-	-
BF-SIFT	39	1.425	0.983
AAG-SIFT	55	1.137	1.013
Proposed Method	**76**	**0.964**	**1.072**

The SIFT-OCT algorithm extracts very less number of features because of its isotropic Gaussian scale space. The isotropic scale space blurs a lot of image details which reduces the number of extracted features. Therefore, the number of correct matches is comparatively less for the SIFT-OCT algorithm. The filtering quality of AAG-SIFT is better than the BF-SIFT. As a result, the AAG-SIFT gives more matches than the BF-SIFT method. However, the gradients are computed by the differential equation for both the methods. The simple differential equation gives stronger gradient value on homogeneous regions with high reflectivity than that with low reflectivity [4]. As a result, it is not appropriate for the gradient calculation in SAR images. In our proposed method, the gradients are computed by the ratio operator which is more effective in SAR images. Therefore, the proposed algorithm gives better performance than the other methods. However, the proposed method has no controllability on the number of extracted features. It extracts around 9000, 4000, 7000 features for the first, second and the third data sets respectively. Moreover, the features are not evenly distributed for all images.

V. CONCLUSION

In this paper, we have investigated the performance of the GSS-BW based ratio operator for SAR image registration. We have proposed the IAG-SIFT algorithm where the gradient of the anisotropic scale space is computed by the GSS-BW based ratio operator. From the experimental results analysis it is obvious that the ratio operator is very effective for gradient computation in the presence of multiplicative speckle noise. As a result, the proposed IAG-SIFT algorithm significantly increases total correct matches between the input images compared to the other algorithms. However, the proposed method does not obtain sub-pixel accuracy for each of data sets as the matches are not uniformly distributed in some cases. The evenly distributed feature extraction algorithm can be adapted to distribute the IAG-SIFT features which can be considered as future work.

REFERENCES

[1] D. G. Lowe, “Distinctive image features from scale-invariant keypoints,” Int. J. Comput. Vis. , vol. 60, no. 2, pp. 91–110, Nov. 2004.

[2] S. Paul and Umesh C. Pati, “Remote sensing optical image registration using modified uniform robust SIFT,” IEEE Geosci. Remote Sens. Lett., vol. 13, no. 9, Sept. 2016.

[3] P. Schwind, S. Suri, P. Reinartz, and A. Siebert ,“Applicability of the SIFT operator for geometrical SAR image registration,” Int. J. Remote Sens., vol. 31, no. 8, pp. 1959–1980, Mar. 2010.

[4] F. Dellinger, J. Delon, Y. Gousseau, J. Michel, and F. Tupin,,“SAR-SIFT: A SIFT-like algorithm for SAR images,” IEEE Trans. Geosci. Remote Sens., vol. 53, no. 1, pp. 453–466, Jan. 2015.

[5] B. Wang, J. Zhang, L. Lu, G. Huang, and Z. Zhao, “A Uniform SIFTLike Algorithm for SAR Image Registration”, IEEE Geosci. Remote Sens. Lett., vol. 12, no. 7, pp. 1426-1430, Jul. 2015.

[6] S. Wang, H. You, and K. Fu,“BFSIFT: A novel method to find feature matches for SAR image registration,” IEEE Geosci. Remote Sens. Lett., vol. 9, no. 4, pp. 649–653, Jul. 2012.

[7] F. Wang, H. You, and X. Fu, “Adapted anisotropic Gaussian SIFT matching strategy for SAR registration,” IEEE Geosci. Remote Sens. Lett., vol. 12, no. 1, pp. 160–164, Jan. 2015.

[8] P. Shui and D. Cheng, “Edge detector of SAR images using GaussianGamma-Shaped Bi-Windows,” IEEE Geosci. Remote Sens. Lett., vol. 9, no. 5, pp. 846–850, Sept. 2012.

[9] M. Chen, Q. Zhu and J. Zhu, “GGSOR: a Gaussian-Gamma-Shaped Bi-Windows based descriptor for optical and SAR images matching,” IEEE Int. Conf. on IGARSS, pp. 3683–3686, 2015.

[10] J. M. Geusebroek, A. W. Smeulders, and J. Van De Weijer, “Fast anisotropic Gauss filtering”, IEEE Trans. Image Process., vol. 12, no. 8, pp. 938–943, Aug. 2003.

[11] [Online]. Available: https://www.asf.alaska.edu/sar-data.

[12] [Online]. Available: https://terrasar-x-archive.terrasar.com.